DIFFERENTIAL MODE DELAY — FULL-WAVE MODELLING AND VARIOUS LEVELS OF APPROXIMATIONS

M. Bingle,[1] **B. P. de Hon**[2]

[1]***Eindhoven University of Technology, Department of Electrical Engineering, P.O. Box 513, 5600 MB Eindhoven, The Netherlands. m.bingle@tue.nl***

[2]***As (1) above, but E-mail:b.p.d.hon@tue.nl***

ABSTRACT

Differential mode delay (DMD) modelling and measurements provide a means to characterise the modal structure of graded-index multimode fibres. In order to compute DMD output time pulses, we need to solve the modal propagation coefficients, modal group velocities and modal chromatic dispersion, compute the weighted modal amplitudes which are dependent on the excitation, and construct time pulses after propagating a specified distance in the fibre. Based on the measurement specifications in the DMD standard [1], we present a robust full-wave numerical approach and discuss various approximations in the modelling of differential mode delay.

INTRODUCTION

For the implementation of networks at 10 Gb/s ethernet and beyond, fast channels are required. In comparison with a single-mode fibre network implementation, a multimode fibre network setting comprises an attractive alternative owing to the ease of connecting a multimode fibre to affordable optical transducers. Unfortunately, the capacity of multimode fibres regarding the bandwidth is significantly limited due to intermodal dispersion. Further, in multimode fibre data transfer measurements isolated modes can neither be excited nor detected, and hence the specific amplitude distribution of the excited modal fields must be incorporated in the definition of the bandwidth.

An overfilled launch by a light-emitting diode comprises an observable measure for the bandwidth, albeit that with the pertaining excitation the specifications cannot be met. Alternatively, the multimode fibre can be connected to a short single-mode fibre that is excited by a laser. Thus, the spot size of the launch is reduced to roughly $5\,\mu\mathrm{m}$. In that setting, the bandwidth can be defined in terms of the differential mode delay (DMD [1, 2]) observed upon gradually moving the single-mode fibre transversely away from the centre of the fibre under test. The pertaining bandwidth can be increased by tuning the refractive-index profile so as to reduce both the travel-time drift of the mode ensemble observed upon increasing the transverse offset, and the pulse broadening due to intermodal dispersion between mode groups.

In numerical modelling for optical fibres, it is common practice to employ the so-called weak guidance approximation. Although that approach is very successful in describing the phenomenology, the severe bandwidth specifications prompt for a cautious attitude. To steer clear of pitfalls regarding DMD simulations, we prefer to commence with an accurate and robust full-wave numerical approach. Subsequently, we discuss the influence on the DMD of neglecting instantaneous-power mode coupling, polarisation-dependent excitation and chromatic dispersion.

FORMULATION OF THE PROBLEM

The multimode fibres under consideration are assumed circularly symmetric, isotropic and translationally invariant. A fibre consists of a radially inhomogeneous core, and a homogeneous cladding of infinite radial extent. The permittivity of the fibre material, $\varepsilon(r,\omega)$ ($e^{j\omega t}$ time-harmonic fields), is characterised by the Sellmeier coefficients for doped, bulk, fibre glass, taken from [3]. The Sellmeier coefficients for a three-term harmonic oscillator model are used; the damping coefficients are neglected to a good approximation in the relevant wavelength bands. We shall present numerical results pertaining to two profiles, depicted in Fig. 1(a).

We employ a vectorial field model to compute the properties of the HE_{mn} and EH_{mn} modes, where $m = 0, 1, 2, \ldots$ and $n = 1, 2, \ldots$ are the azimuthal and radial modal indices, respectively. In circularly cylindrical coordinates the modal field

[1]M. Bingle thankfully acknowledges the financial support received from *Draka Fibre Technology BV*.

[2]B. P. de Hon thankfully acknowledges the fellowship grant from the *Royal Netherlands Academy of Arts and Sciences*.

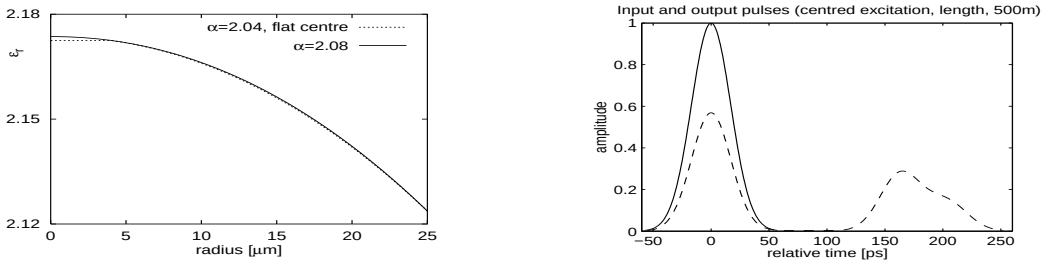

(a) (b)

Fig. 1. The solid and dotted lines in (a) show a power-law profile, ($\varepsilon = \varepsilon_0(1 - 2\Delta\rho^\alpha)$), and a power-law profile with a flat centre, respectively. In (b) the input and output pulses for centred excitation of the flat-centre fibre are shown.

components in a z-directed fibre can be expressed as,

$$\{\hat{H}_\varphi^{mn}, \hat{E}_z^{mn}, \hat{E}_r^{mn}\} = 2\rho^{|m|}\{Y_0\rho^{-1}h_\varphi^{mn}, e_z^{mn}, \rho^{-1}e_\rho^{mn}\}\cos(m\varphi - \varphi_0^{mn})e^{-jk_z^{mn}z}, \tag{1a}$$

$$\{\hat{E}_\varphi^{mn}, \hat{H}_z^{mn}, \hat{H}_r^{mn}\} = 2\rho^{|m|}\{\rho^{-1}e_\varphi^{mn}, Y_0 h_z^{mn}, \rho^{-1}Y_0 h_\rho^{mn}\}\sin(m\varphi - \varphi_0^{mn})e^{-jk_z^{mn}z}, \tag{1b}$$

where k_z^{mn} is the propagation coefficient and $\rho = r/a$ is the radial coordinate normalised to the core radius a. Substituting (1) in the source-free Maxwell's equations yields a system of coupled, first-order, ordinary, differential equations (cf. [4]),

$$\frac{\mathrm{d}}{\mathrm{d}\rho}\mathbf{f}(\rho) = \rho^{-1}\mathsf{A}(\rho)\mathbf{f}(\rho), \quad \text{with} \quad \mathbf{f}(\rho) = [e_\varphi(\rho)\ \ e_z(\rho)\ \ h_\varphi(\rho)\ \ h_z(\rho)]^T, \tag{2}$$

for each mode. The field vector $\mathbf{f}(\rho) = \mathbf{f}^{mn}(\rho)$ is real for lossless media. Two independent field solutions remain bounded for $\rho \downarrow 0$. Starting with the bounded field solutions at $\rho = 0$, (2) is integrated numerically (cf. [5]) to a suitably chosen radius, $\rho_{m;\mathrm{tp}}$. Typically, we choose $\rho_{m;\mathrm{tp}}$ to be a turning point associated with m. The two field solutions that remain bounded in the cladding are expressed in terms of modified Bessel functions; these field solutions are integrated to $\rho_{m;\mathrm{tp}}$ as well. Imposing the continuity conditions across $\rho_{m;\mathrm{tp}}$ leads to a characteristic equation, $C_{m;\mathbf{f}}(\omega, \zeta) \equiv 0$ (with ω and m fixed), for the normalised, modal propagation coefficients, $\zeta = \zeta^{mn} = k_z^{mn}c_0/\omega$.

For differential mode delay computations, the modal group delay times, $\tau_g^{mn} = \mathrm{d}k_z^{mn}/\mathrm{d}\omega$, are of importance. Depending on the excitation linewidth and the fibre length, the first order chromatic (intramodal) dispersion might also be relevant. Chromatic dispersion is defined per fibre length, L, in terms of the first derivative of the modal group delay with respect to the vacuum wavelength, λ. In order to compute the (higher-order) derivatives of k_z^{mn} accurately, we consider multiple total derivatives of the characteristic equation with respect to ω. Since all total derivatives of the characteristic equation vanish identically, e.g. $\mathrm{d}C_{m;\mathbf{f}}/\mathrm{d}\omega = (\mathrm{d}\zeta/\mathrm{d}\omega)\partial_\zeta C_{m;\mathbf{f}} + \partial_\omega C_{m;\mathbf{f}} \equiv 0$, relations can be obtained for the derivatives of ζ with respect to ω, e.g. $\mathrm{d}\zeta/\mathrm{d}\omega = -\partial_\omega C_{m;\mathbf{f}}/\partial_\zeta C_{m;\mathbf{f}}$, from which the group delay can be computed. The partial derivatives of $C_{m;\mathbf{f}}$ are constructed from partial derivatives of the field vector at $\rho = \rho_{m;\mathrm{tp}}$. To this end, an extended system of coupled, ordinary, differential equations for $\mathbf{f}(\rho)$ and its required partial derivatives was derived from (2), [6]. The extended system is integrated numerically, analogous to (2). We have found this method to be robust and accurate in the computation of the higher order derivatives of ζ. Alternatively, we could have employed an impedance-angle formalism (cf. [7]), which leads to a characteristic equation, $C_{m;\mathbf{\Phi}}(\omega, \zeta) \equiv 0$, that is convenient for mode counting. However, the expressions for the partial derivatives of the associated system of ordinary non-linear differential equations are far more intricate.

EXCITATION OF THE MODAL FIELD

Since the modes propagate along the z-direction, it is convenient to arrange the time-harmonic field components that are transverse to the z-direction in a vector according to $\hat{\mathbf{F}} = (\hat{E}_r\ \ \hat{E}_\varphi\ \ \hat{H}_\varphi\ \ \hat{H}_r)^T$. Further, we define a power-flow product between two electromagnetic states with transverse vectors $\hat{\mathbf{F}}^{\mathrm{A}}$ and $\hat{\mathbf{F}}^{\mathrm{B}}$ according to

$$\langle\hat{\mathbf{F}}^{\mathrm{A}}, \hat{\mathbf{F}}^{\mathrm{B}}\rangle = \frac{1}{2}\int_{\mathbb{R}^2}\mathbf{u}_z \cdot \left[\hat{\mathbf{E}}^{\mathrm{A}} \times (\hat{\mathbf{H}}^{\mathrm{B}})^*\right]\,\mathrm{d}A. \tag{3}$$

Once the modal field vectors have been computed, the fields are normalised such that $\langle\hat{\mathbf{F}}^{m'n'}, \hat{\mathbf{F}}^{mn}\rangle = \delta_{m',m}\delta_{n',n}$, where $\delta_{m',m}$ denotes the Kronecker delta. In principle, one would have to solve a scattering problem in order to determine the modal field distribution excited in the multimode fibre at the splice with the single-mode fibre probe. In practice, this

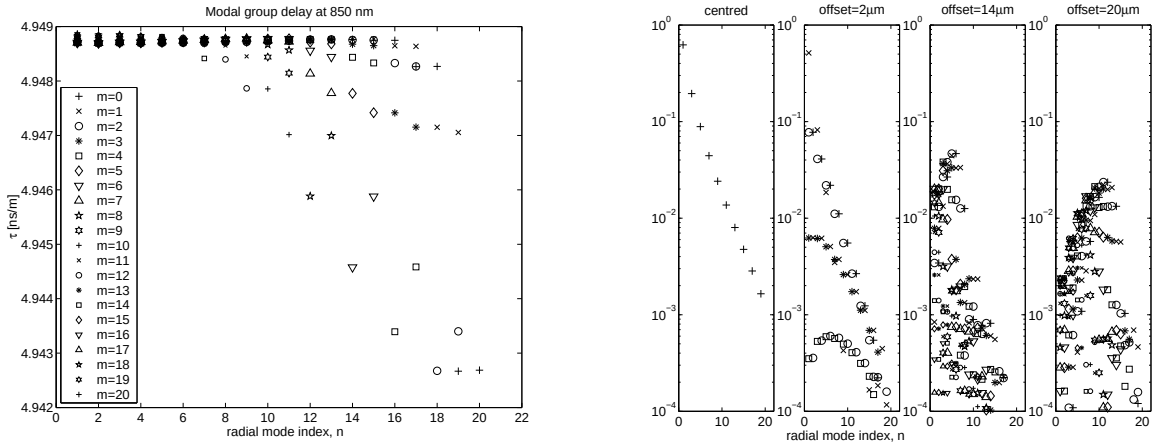

(a) (b)

Fig. 2. The modal group delays for the power-law profile (a), and the excited modal amplitudes for four probe offsets (b).

splice is seldom perfect, and hence full-wave scattering results would be of little practical importance. Furthermore, the contrast between fibres is so small that it suffices to project the (single-mode) probe field $\hat{\mathbf{F}}^{\mathrm{i}}$ onto the modal fields in the multimode fibre with the aid of overlap integrals [8, pp. 170–174],

$$Q^{mn} = \langle \hat{\mathbf{F}}^{\mathrm{i}}, \hat{\mathbf{F}}^{mn} \rangle = \frac{1}{2} \int_{\rho=0}^{\infty} \int_{\varphi=0}^{2\pi} \mathbf{u}_z \cdot \left\{ \hat{\mathbf{E}}^{\mathrm{i}}(\rho', \varphi') \times [\hat{\mathbf{H}}^{mn}(\rho, \varphi)]^* \right\} \, \rho \, \mathrm{d}\varphi \, \mathrm{d}\rho, \tag{4}$$

where Q^{mn} denotes the modal amplitude of the corresponding excited mode, and $\{\rho', \varphi'\} = \{\rho'(\rho, \varphi), \varphi'(\rho, \varphi)\}$ denote the transverse cylindrical polar coordinates about the probe axis. In (4), the Fourier integral along φ can be evaluated prior to the determination of the radial modal fields of the multimode fibre. It is computed with the aid of an adaptive quadrature routine. For the integral along ρ a fixed quadrature rule suffices. The distribution of the power among the different modes will also be affected by the differential mode attenuation, primarily due to bending losses. Differential mode attenuation has not been incorporated into the numerical model.

THE RECEIVED TIME SIGNAL

At the receiver end of the fibre, the transmitted signals are detected by a power sensor, which measures the total *instantaneous* power $P = \int_{\mathcal{D}} \mathbf{u}_z (\cdot \mathbf{E} \times \mathbf{H}) \, \mathrm{d}A$ flowing through a cross-section. Due to speed limitations, only the moving time average of P is recorded. Fig. 1(b) shows an example of aligned input and output power pulses. The instantaneous power corresponds to a convolution in the frequency domain. In general modes at different frequencies are not orthogonal. Hence, the power of modes associated with equal m, but different n couple. Further, for off-centred excitation the rotational symmetry with respect to the probe polarisation is broken. Hence, for probes excited by sources with design-dependent polarisation properties, e.g. vertical-cavity surface-emitting lasers, one might expect probe-polarisation dependent DMD results. However, for the practical small-contrast multimode fibre setting under consideration, these effects on the DMD are so weak that the differences between the "exact" results and the ones for which instantaneous-power mode coupling is neglected and probe-polarisation asymmetry is ignored, do not warrant a separate graph. For the DMD examples discussed below, the 25% pulsewidth, $T = 56.57$ ps and fibre length, $L = 500$ m, are such that $D \ll \pi c T^2/(2L\lambda^2 \log 4)$, and hence the chromatic dispersion may safely be neglected. However, sources generating multiple lasing modes should be avoided, since a distribution of several spectral lines does lead to a severe increase in the chromatic dispersion. For the numerical simulation of DMD experiments conducted according to the DMD standard [1], it suffices to calculate the excited modal amplitudes and the modal group delays (cf. Fig. 2). Assuming an optimal resolution of the time window of observation of a few picoseconds, a relative accuracy of about 10^{-6} is required for the calculation of $\tau_{\mathrm{g}} = \mathrm{d}k_z/\mathrm{d}\omega$. Regarding the sum of the modal amplitudes, an accuracy of 10^{-2} is sufficient.

DMD RESULTS

It has been reported [2] that fibres with a power profile, $\varepsilon = \varepsilon_0(1 - 2\Delta\rho^{\alpha}), \ \rho \in [0, 1]$, may exhibit a good overall DMD behaviour (i.e. a minimum travel-time drift for different probe offset positions, and minimum pulse distortion.) Via

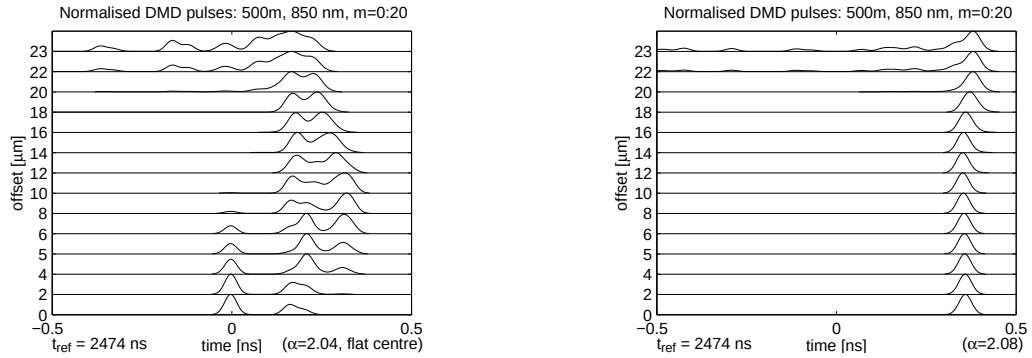

(a) (b)

Fig. 3. DMD results for the flat-centre power-law profile (a) and the power-law profile (b).

adjustment of the α-parameter, an optimal DMD-response can be obtained. The modal group delays for a power-law profile are depicted in Fig. 2. The associated modal amplitude distribution shows that only a selection of modes are excited with significant amplitudes at various offsets. Inspection of the corresponding DMD in Fig. 3(b), reveals only a slight travel-time drift for large probe offsets. At an optimum (in this case, slightly smaller) α, the DMD output pulses will align. The result for the flattened power-law profile, Fig. 3(a), shows the combined effect of a non-optimal value for α and a profile deviation on the DMD output pulses. We infer from the earlier arrivals for larger offsets that the value of α is too small. Further, Fig. 3(a) indicates that a local deviation from a power profile (viz. a flattened centre) leads to local intermodal dispersion between different mode groups. The effects of profile variations on the DMD characteristics of multimode fibres have been observed experimentally. The numerical computations help to isolate the effect of various profile deviations and emphasize the need for accurate control of the fibre profile in the manufacturing process.

CONCLUSION

The differential mode delay (DMD) of a fibre is the combined effect of the travel-time drift for different probe offset positions and the pulse broadening due to intermodal dispersion between mode groups. By tuning a power-law refractive-index profile, it is possible to design fibres with good DMD characteristics. In view of the sensitivity of the differential mode delay to small profile deviations, the manufacturing process should be very precise. In the numerical simulation of the standard DMD measurement setup, chromatic dispersion, instantaneous-power mode coupling and probe-polarisation asymmetry may safely be neglected. For modes close to cut-off, the neglected effects tend to be stronger. However, these modes are weakly excited in DMD experiments and will in practice be attenuated due to bending losses. Nevertheless, to achieve sufficiently accurate results, the modal group delays and amplitudes should be computed with due care.

REFERENCES

[1] TIA, “FOTP-220 – differential mode delay measurement of multimode fiber in the time domain,” TIA-455-220, PN3-0008, 2001.

[2] P. Pepeljugoski, D. Kuchta, Y. Kwark, P. Pleunis, and G. Kuyt, “15.6 Gb/s transmission over 1km of next generation multimode fiber,” *Proc. 27th Eur. Conf. on Opt. Comm.*, paper We.P.31, 2001, Amsterdam, The Netherlands.

[3] W. Hermann and D. U. Wiechert, “Refractive index of doped and undoped PCVD bulk silica,” *Mat. Res. Bull.*, vol. 24, p. 1083, 1989.

[4] J. G. Dil and H. Blok, “Propagation of electromagnetic surface waves in a radially inhomogeneous optical waveguide,” *Opto-electronics*, vol. 5, pp. 415–428, 1973.

[5] A. G. Tijhuis and R. M. van der Weiden, “SEM approach to transient scattering by a lossy, radially inhomogeneous dielectric circular cylinder,” *Wave motion*, vol. 8, pp. 43–63, 1986.

[6] M. Bingle, B. P. De Hon, and M. J. N. van Stralen, “Electromagnetic modelling and optimisation for the design of single-mode optical fibres,” *Proc. 2001 URSI Int. Symposium on Electromagnetic Theory,* Victoria, Canada, pp. 515–517, 2001.

[7] B.P. de Hon and M. Bingle, “A modal impedance-angle formalism — schemes for accurate graded-index bent-slab calculations and optical fibre mode counting,” unpublished.

[8] E.-G. Neumann, *Single-Mode Fibers, Fundamentals.* Berlin: Springer, 1988.